portant polyhedra with n vertices can often be surprising small, particularly when $|Q_n|$ is considered relative to $n!$. For example, a group $Q_9 = P_2[P_3]$[2] with only 72 elements has been found which spans the symmetries of all of the chemically feasible nine-vertex polyhedra just as well as the much larger group P_9 with 9! = 362 880 elements. It thus appears that use of the Q_n subgroups rather than the fully symmetrical P_n group might offer some advantages of simplicity in depiciting isomerization processes in stereochemically nonrigid polyhedra. Applications of these principles to permutational isomerisms in eight-coordinate ML_8 complexes are currently under investigation.

Contribution from the Department of Chemistry, University of Maine, Orono, Maine 04469, and the Department of Physics, Brookhaven National Laboratory, Upton, New York 11973

Pure- and Mixed-Crystal Optical Studies of the Jahn-Teller Effect for the d^6 Hexafluoroplatinate(IV) Ion

MICHEL P. LAURENT, HOWARD H. PATTERSON,* WILLIAM PIKE, and HERBERT ENGSTROM

Received May 1, 1980

Measurements have been made of the low-temperature luminescence and Raman spectra of pure Cs_2PtF_6 crystals and Cs_2PtF_6–Cs_2GeF_6 crystals in which PtF_6^{2-} is doped into the Cs_2SiF_6 lattice. In both environments, the Raman spectra at liquid-helium temperature show sharp lines assigned to the a_{1g}, e_g, and t_{2g} internal modes of the PtF_6^{2-} ion. A comparison of the low-temperature Raman and sharp-line luminescence spectra indicates that in the luminescence spectra a Jahn–Teller e_g-type progression occurs with a small degree of anharmonicity present. The luminescence can be assigned as a transition from the $t_{2g}^5e_g\ \Gamma_3(^3T_{1g})$ twofold degenerate excited electronic state to the $t_{2g}^6\ \Gamma_1(^1A_{1g})$ nondegenerate ground electronic state.

Introduction

MX_6^{2-} octahedral hexahalide systems, where M is a 5d transition-metal element, have been the subject of numerous optical studies in recent years.[1] The optical measurements have almost always been mixed-crystal experiments in which the MX_6^{2-} impurity ion is doped in a cubic host such as Cs_2ZrCl_6, Cs_2ZrBr_6, or Cs_2SiF_6 and the optical spectrum is recorded at liquid-helium temperature. It is important to compare the pure-crystal spectra with the impurity ion results. In this paper we report Raman and luminescence experiments for the d^6 PtF_6^{2-} ion in the pure Cs_2PtF_6 case and in the case where the PtF_6^{2-} ion is doped in a host lattice. In particular, the d^6 PtF_6^{2-} ion is an excellent ion to study for two reasons: (1) the PtF_6^{2-} ion in both the pure- and mixed-crystal environments shows strong structured luminescence spectra; (2) the Raman spectra in both the pure and mixed crystals show lines due to the Raman-active a_{1g}, e_g, and t_{2g} modes of the PtF_6^{2-} moiety.

In a previous publication on the PtF_6^{2-} ion,[2] the luminescence spectra were assigned to an a_{1g} progression because of limited data. In these current studies the luminescence spectra were recorded with an infrared optical system and Raman spectra measured at liquid-helium temperature. Also, lifetime studies have been performed in both the pure- and mixed-crystal cases as a function of temperature. Comparison of the luminescence and Raman spectra now leads to a model in which in the luminescence spectra an e_g Jahn–Teller-active progression occurs. The decreasing spacing between the luminescence peaks with decreasing energy is explained by a small degree of anharmonicity in the ground-electronic-state potential surface for the e_g mode.

Experimental Section

The synthesis of Cs_2PtF_6 and the growing of crystals (Cs_2PtF_6; Cs_2PtF_6–Cs_2SiF_6, Rb_2PtF_6–Rb_2SiF_6) have been discussed previously.[2] The analysis of the Rb_2PtF_6–Rb_2SiF_6 and Cs_2PtF_6–Cs_2SiF_6 mixed crystals was carried out by R. W. Stoenner of the Chemistry Department at Brookhaven. The percent Pt was determined by a flameless-graphite-furnace atomic absorption at 2800 °C by standard addition. The percent Si was determined spectrophotometrically with a Cary Model 16 by using the method of Andrew[3] in which ammonium molybdate complexes with silicon to give an absorption band at 810 nm. The results for the actual crystal batch used for the Raman studies showed that for the Rb_2PtF_6–Rb_2SiF_6 mixed crystals the relative amount of Rb_2PtF_6 was 1.3% while for the Cs_2PtF_6–Cs_2SiF_6 crystals the relative amount of Cs_2PtF_6 was 7.9%.

The emission studies were performed by exciting the crystal samples with a Molectron UV 14 nitrogen laser. The resulting luminescence was analyzed with a McPherson 1-m Model 2051 monochromator and a Products for Research TE-241-RF photomultiplier tube. Emission spectra were recorded after amplification of the signal with a PAR 124A lock-in amplifier. Lifetime measurements were made with a PAR boxcar averager, Model 162. In all cases the sample temperatures were obtained with an Lt-3-110 liquid-helium transfer Heli-Tran.

Raman measurements were made with the use of a krypton ion laser excitation at 476.2, 530.9, and 568.2 nm. The details of the detection system have been published.[4] The absorption measurements at liquid-helium temperature were performed with a Cary 17D spectrophotometer.

Results

Emission Spectra. Luminescence measurements were made on single crystals of Cs_2PtF_6, Cs_2PtF_6–Cs_2SiF_6, Cs_2PtF_6–Cs_2GeF_6, and Rb_2PtF_6–Rb_2SiF_6 with excitation at 337.1 nm. Intense emission as a yellow-orange glow is observed in every case even at room temperature. At room temperature only a broad featureless band is observed with the maximum in each case: Cs_2PtF_6, 648.0 ± 3 nm; Cs_2PtF_6–Cs_2SiF_6 and Cs_2PtF_6–Cs_2GeF_6, 620.0 ± 2 nm; and Rb_2PtF_6–Rb_2SiF_6, 600.0 ± 2 nm. At 5 K well-resolved structure appears. The luminescence spectra at 5 K of a pure Cs_2PtF_6 crystal and a mixed Cs_2PtF_6–Cs_2SiF_6 crystal are shown in Figures 1 and 2, respectively.

Emission Lifetime Measurements. These were performed on single crystals of Cs_2PtF_6, Cs_2PtF_6–Cs_2SiF_6, Cs_2PtF_6–

* To whom correspondence should be addressed at the University of Maine.

(1) Selected representative papers: (a) P. B. Dorain and R. G. Wheeler, *J. Chem. Phys.*, **45**, 1142 (1965); (b) P. B. Dorain, H. H. Patterson, and P. C. Jordan, *ibid.*, **49**, 3854 (1968); (c) J. C. Collingwood, S. B. Piepho, R. W. Schwartz, P. A. Dobosh, J. R. Dickinson, and P. N. Schatz, *Mol. Phys.*, **29**, 793 (1975); (d) H. H. Patterson, J. L. Nims, and C. M. Valencia, *J. Mol. Spectrosc.*, **42**, 567 (1972); (e) L. Lindsay Helmholtz and M. E. Russo, *J. Chem. Phys.*, **59**, 5455 (1973).
(2) H. H. Patterson, W. J. DeBerry, J. E. Byrne, M. T. Hsu, and J. A. LoMenzo, *Inorg. Chem.*, **16**, 1698 (1977).
(3) T. R. Andrew, *Analyst (London)*, **82**, 423 (1957).
(4) H. Engstrom, *Rev. Sci. Instrum.*, **47**, 928 (1976).

0020-1669/81/1320-0372$01.00/0

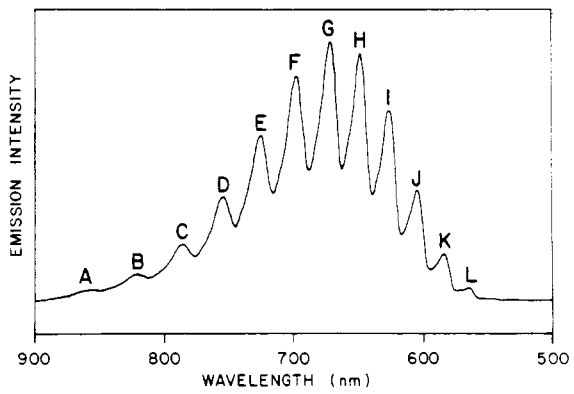

Figure 1. Luminescence spectrum of a single Cs_2PtF_6 crystal at 5 K.

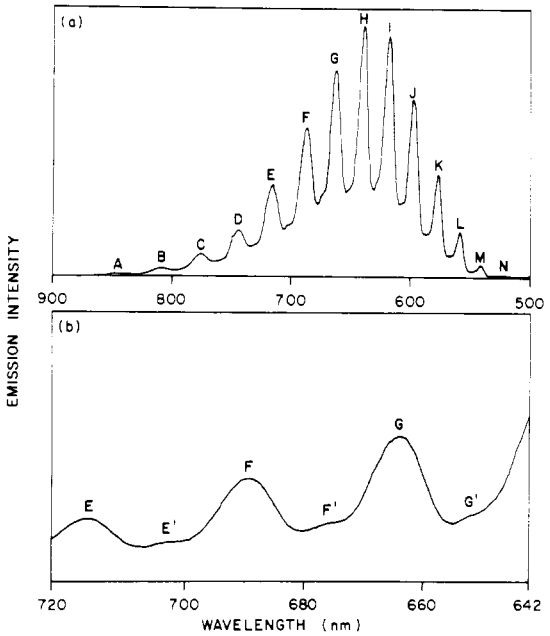

Figure 2. Luminescence spectrum of a Cs_2PtF_6–Cs_2SiF_6 mixed crystal at 5 K. The lower figure (b) shows the low intensity peaks observed in the luminescence spectrum and denoted by primes.

Table I. Intercept and Slope of the Line Fitted to the Points in a Plot of Emission Half-Life vs. Temperature for Cs_2PtF_6, Cs_2PtF_6-Cs_2SiF_6, Cs_2PtF_6-Cs_2GeF_6, Rb_2PtF_6-Rb_2SiF_6

crystal	intercept,[a] μs	μs/K	temp range,[b] K
Cs_2PtF_6	3570	11	5–293
$Cs_2(Pt,Si)F_6$	4340	7.5	7–290
$Cs_2(Pt,Ge)F_6$	4340	7.4	5–290
$Rb_2(Pt,Si)F_6$	3860	8.7	78–290

[a] It is the linearly extrapolated half-life at 0 K. [b] Range of temperatures over which the luminescence decay was studied.

Cs_2GeF_6, and Rb_2PtF_6–Rb_2SiF_6 at various temperatures. The excitation wavelength was 337.1 nm, while the monitoring wavelength was in the neighborhood of the band maximum. The emission decay rates were found to obey the first-order rate law

$$dI/dt = I/\tau \quad (1)$$

where I is the emission intensity at time t and τ is the mean lifetime. A plot of the half-life of emission, $t_{1/2} = \tau \ln 2$, vs. temperature is shown for Cs_2PtF_6–Cs_2SiF_6 in Figure 3. Table I gives the values of the intercept and slope of the lines obtained for each system. As expected, the lifetimes increase with decreasing temperature. It is also seen that the magnitude

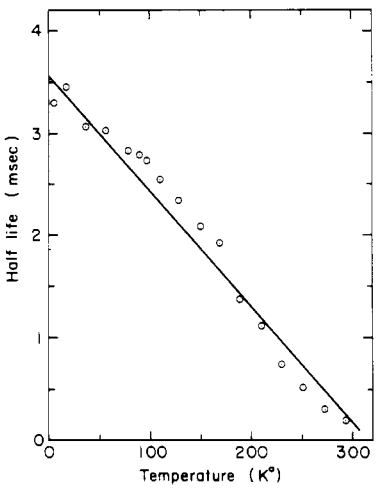

Figure 3. Plot of emission half-life vs. temperature for a typical Cs_2PtF_6–Cs_2SiF_6 crystal.

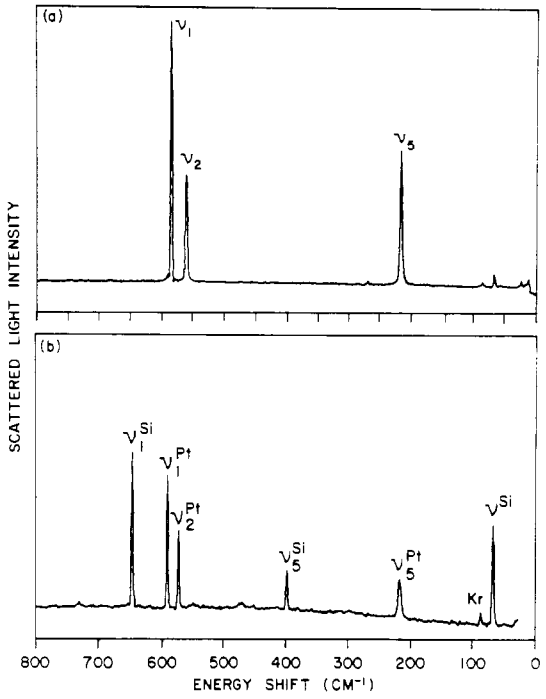

Figure 4. Raman spectra of (a) a Cs_2PtF_6 crystal and (b) a Cs_2PtF_6–Cs_2SiF_6 crystal, both at 5 K with λ(excitation) = 530.9 nm.

of the lifetimes are dependent on the environment of the PtF_6^{2-} ion. Cs_2PtF_6 exhibits the shortest lifetimes and the greatest decrease in lifetime per Kelvin. Cs_2PtF_6–Cs_2SiF_6 and Cs_2PtF_6–Cs_2GeF_6 behave nearly identically, but they exhibit lifetimes a factor of 10 longer than Cs_2PtF_6 at room temperature. Rb_2PtF_6–Rb_2SiF_6 is intermediate in behavior between Cs_2PtF_6 and the other mixed crystals. Toward lower temperatures these differences in the lifetime values among the crystals decrease, and the linearly extrapolated half-life at 0 K is about 4 ms in each case (Table I). It is also of interest that for Cs_2PtF_6 the emission half-lives at 565.7, 625.4, 672.0, and 786.4 nm are equal within experimental error, consistent with no dependence of the emission decay rate on wavelength.

Raman Measurements. Raman spectra at 4 K were obtained for single crystals of Cs_2PtF_6 (Figure 4a) and Cs_2PtF_6–Cs_2SiF_6 (Figure 4b). Assignments and energies are summarized in Table II.

Jahn–Teller Model

The liquid-helium Raman spectra of a pure Cs_2PtF_6 crystal, shown in Figure 4a, has peaks at 220, 566, and 590 cm^{-1}. On

Table II. Summary of Raman Measurements for Cs_2PtF_6, Cs_2PtF_6–Cs_2SiF_6, and Cs_2SiF_6 at 4 K

	vib mode energy, cm^{-1}			
		$Cs_2(Pt,Si)F_6$		
vib mode	Cs_2PtF_6	Pt	Si	Cs_2SiF_6[a]
$\nu_1(a_{1g})$	591.3	591.3	647.3	647
$\nu_2(e_g)$	565.7	573.3		469
$\nu_5(t_{2g})$	221	217.7	399.3	401
lattice			67.5[b]	68.8[b]

[a] Data from ref 6. [b] Arises from Cs^+ motion.

the basis of previous polarized Raman studies at room temperature,[5] we assign these peaks to the $\nu_5(t_{2g})$, $\nu_2(e_g)$, and $\nu_1(a_{1g})$ vibrational modes of the PtF_6^{2-} ion, respectively. The Raman spectrum of a Cs_2PtF_6–Cs_2SiF_6 crystal at liquid-helium temperature has peaks due to both SiF_6^{2-} and PtF_6^{2-} internal modes, as shown in Figure 4b. We have previously studied the Cs_2SiF_6 vibrational Raman spectrum at 5 K,[6] and, thus, we can assign these mixed-crystal peaks. The PtF_6^{2-} mode energies for a Cs_2PtF_6–Cs_2SiF_6 crystal at liquid-helium temperature are $\nu_5 = 218$, $\nu_2 = 573$, and $\nu_1 = 591$ cm^{-1}.

The luminescence spectrum of a pure Cs_2PtF_6 crystal at liquid-helium temperature (see Figure 1) shows a progression of peaks with an average spacing of 551 cm^{-1}. This energy is not equal to the ν_1, ν_2, or ν_5 mode energies but is certainly closer to ν_2 than to ν_1. For a crystal at liquid-helium temperature, before luminescence occurs, there should only be an appreciable Boltzmann population of the excited electronic state lowest vibronic levels. Thus, we propose that the observed luminescence structure is due to a progression in the ground electronic state PtF_6^{2-} $\nu_2(e_g)$ vibrational mode with the energy of v $\nu_2(e_g)$ vibrational quanta given by[7] eq 2. It is assumed

$$E(v) = W_e(v + 1) - W_eX_e(v + 1)^2 \qquad (2)$$

that the observed highest energy luminescence peak corresponds to the $v = 0$ state. A least-squares fit of the Cs_2PtF_6 luminescence peak energies to eq 2 gives $W_e = 570 \pm 3$ cm^{-1} and $\overline{W_eX_e}$, the anharmonic correction to a harmonic oscillator, equal to 1.65 ± 0.14 cm^{-1}. In contrast, a least-squares fit of the Cs_2PtF_6–Cs_2SiF_6 liquid-helium luminescence data yields $W_e = 579 \pm 6$ cm^{-1} and $\overline{W_eX_e} = 1.88 \pm 0.32$ cm^{-1} in comparison to the Raman ν_2 value of 573 cm^{-1}. We conclude there is reasonable agreement between the ν_2 Raman values and the ν_2 values obtained from the luminescence spectra fit to eq 2.

Crystal field calculations for the d^6 PtF_6^{2-} ion,[2] with inclusion of spin–orbit interaction, show that the lowest energy excited electronic state is $\Gamma_3(^3T_{1g})$, where Γ_3 is a twofold degenerate irreducible representation. This result is true for a wide range of crystal field parameters. Thus, the luminescence spectrum is assigned to a transition between the $t_{2g}^5e_g$ $\Gamma_3(^3T_{1g})$ state and the t_{2g}^6 $\Gamma_1(^1A_{1g})$ ground electronic state.

The Hamiltonian for the linear Jahn–Teller coupling of a doubly degenerate electronic state to a doubly degenerate e_g vibration for a symmetrical nonlinear molecule is given by[8-10] eq 3 with I being a 2×2 unit matrix. The resulting vibronic

$$\mathcal{H} = -\frac{1}{2}\left[\frac{\partial^2}{\partial r^2} + \frac{1}{r}\frac{\partial}{\partial r} + \frac{1}{r^2}\frac{\partial^2}{\partial \phi^2} - r^2\right]\hat{I} + \begin{bmatrix} 0 & Kre^{-i\phi} \\ Kre^{i\phi} & 0 \end{bmatrix} \qquad (3)$$

Table III. Luminescence Spectra of a Cs_2PtF_6 Single Crystal and a Cs_2PtF_6–Cs_2SiF_6 Crystal at 5 K

Bands for Cs_2PtF_6

				rel intens	
band	λ, nm	ν, cm^{-1}	$\Delta\nu$, cm^{-1}	exptl	calcd
A	859.3	11 637	531	4.5	10
B	821.8	12 168	548	11	19
C	786.4	12 716	534	23	32
D	754.7	13 250	547	41	50
E	724.8	13 797	534	65	71
F	697.8	14 331	550	89	90
G	672.0	14 881	551	100	100
H	648.0	15 432	558	94	96
I	625.4	15 990	556	71	79
J	604.4	16 545	575	42	52
K	584.1	17 120	547	18	28
L	566.0	17 668	583	5.0	9
M	547.9	18 252		0.7	2

High-Intensity Bands for Cs_2PtF_6–Cs_2SiF_6

				rel intens	
band	λ, nm	ν, cm^{-1}	$\Delta\nu$, cm^{-1}	exptl	calcd
A	847.2	11804	583	1.1	4
B	807.3	12387	501	3.1	8
C	775.9	12888	529	8.7	16
D	745.3	13417	549	18	29
E	716.0	13966	541	35	46
F	689.3	14507	566	58	67
G	663.4	15074	590	82	87
H	638.4	15664	512	100	100
I	618.2	16176	576	97	100
J	596.9	16752	558	72	84
K	577.7	17310	576	41	57
L	559.1	17886	573	18	31
M	541.7	18459	582	5.4	11
N	525.2	19040		1.7	3

Low-Intensity Bands for Cs_2PtF_6–Cs_2SiF_6

band	description[a]	λ, nm	ν, cm^{-1}	$\Delta\nu$, cm^{-1}
A′	sh	830.2	12045	527
B′	w sh	795.4	12572	506
C′	sh	764.6	13079	579
D′	vw sh	732.2	13657	554
E′	sh	703.7	14211	578
F′	sh	676.2	14789	549
G′	w sh	652.0	15337	561
H′	w sh	629.0	15898	549
I′	vw sh	608.0	16447	580
J′	flatness	587.3	17027	569
K′	flatness	568.3	17696	579
L′	vw sh	550.2	18175	622
M′	flatness	532.0	18797	

[a] The abbreviations: v, very; w, weak; sh, shoulder.

energy levels can be classified by a quantum number l and a dimensionless parameter K^2 measuring the magnitude of the electronic–vibrational coupling. Note in eq 3 that when $K^2 = 0$ the equation reduces to that of a two-dimensional harmonic oscillator. The selection rules[8] for transitions from the excited-state vibronic levels to a nondegenerate ground electronic state allow excitation of any number of e_g quanta, as though the Jahn–Teller effect is equivalent to a distortion which makes vibrational transitions allowed which are otherwise forbidden.[9]

Longuet-Higgins et al.[10] have transformed eq 3 into an infinite matrix which can be solved by numerical methods. We have written a computer program to solve these secular equations for a range of K^2 J–T parameter values. We have calculated the relative intensities of the v e_g ($\nu = 1, 2, 3, \ldots$) progression members as a function of the parameter K^2 and determined the K^2 value which gives the best least-squares fit of the calculated relative intensities with the experimental data.

(5) Y. M. Bosworth and R. J. H. Clark, *J. Chem. Soc. A*, 1749 (1974).
(6) H. H. Patterson and J. W. Lynn, *Phys. Rev. B: Condens. Matter*, **19**, 1213 (1979).
(7) G. Herzberg, "Electronic Spectra and Electronic Structure of Polyatomic Molecules", Van Nostrand, Princeton, N. J., 1966.
(8) H. C. Longuet-Higgens, U. Opik, M. H. L. Pryce, R. A. Sack, *Proc. R. Soc. London, Ser. A*, **244**, 1 (1958).
(9) R. Englman, "The Jahn-Teller Effect in Molecules and Crystals", Wiley-Interscience, New York, 1972, p 20.
(10) H. C. Longuet-Higgins, *Adv. Spectrosc.*, **2**, 429 (1961).

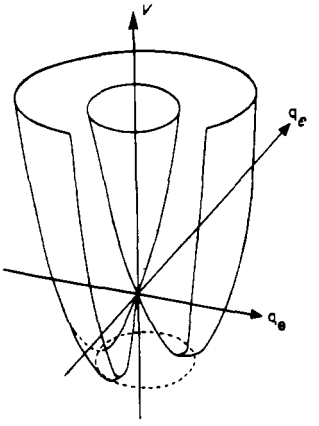

Figure 5. Schematic illustration of the Jahn–Teller potential surface for an E_g electronic state coupled to a e_g vibrational mode. The depth of the well below the origin is calculated to be 3725 cm^{-1} for the Cs_2PtF_6–Cs_2SiF_6 case.

This is straightforward because the vibronic eigenfunctions are expressed as a linear combination of harmonic oscillator eigenfunctions centered at $r = 0$. A summary of the experimental and calculated luminescence results is presented in Table III.

From the Cs_2PtF_6–Cs_2SiF_6 luminescence analysis, we obtain a value of 13.0 for the J–T coupling parameter K^2; this corresponds to a Jahn–Teller well depth of 3725 cm^{-1} as shown in Figure 5. Further, the computer calculations show that the $\Gamma_1(^1A_{1g}) \rightarrow \Gamma_3(^3T_{1g})$ absorption spectrum should consist of two absorption maxima separated by about 3000 cm^{-1} with this value dependent upon the $\Gamma_3(^3T_{1g})$ e_g mode energy. Also, analysis of the pure Cs_2PtF_6 crystal luminescence data yields the result that $K^2 = 13.4$.

Let us now determine the geometry of the PtF_6^{2-} ion while in the $\Gamma_3(^3T_{1g})$ excited state. The $\Gamma_3(^3T_{1g})$ e_g potential surface consists of two potential wells displaced by a value of K from the origin in $Q\theta$,$Q\epsilon$ space. One can calculate the value of displacements in the well minima from the origin by making use of eq 4[11] to convert the unitless variable q to the symmetry

$$Q = (K/\mu w)^{1/2}q \qquad (4)$$

coordinate Q in Å units. This yields $Q_{E\theta} = Q_{E\epsilon} = 0.190$ Å. The transformation of symmetry-coordinate displacements to bond length changes in the X, Y, Z directions has been discussed by Solomon and co-workers.[12] From eq 21 of ref 12 we obtain the result that in the $\Gamma_3(^3T_{1g})$ Jahn–Teller excited state the PtF_6^{2-} ion has tetragonal geometry with the F atoms in the equatorial plane expanded by 0.11 Å and the F atoms in the axial direction compressed by 0.055 Å in comparison to the $\Gamma_1(^1A_{1g})$ ground electronic state.

Lifetime Measurements. Douglas et al.[13] have reported luminescence measurements for K_2PtBr_6 and some $PtCl_6^{2-}$ salts. For K_2Cl_6, the band shape of the luminescence band suggested there might be more than one band present; further, study of the luminescence decay gave two decay times of about 3×10^{-4} and 8×10^{-4} s. This means that in the platinum(4+) chloride salts the spacing between the Γ_3 vibronic Jahn–Teller states is small enough to give appreciable Boltzmann population of more than one level and, thus, give rise to two decay times. In contrast, for PtF_6^{2-} our lifetime measurements vs. temperature indicate that the observed luminescence occurs from only one emitting state.

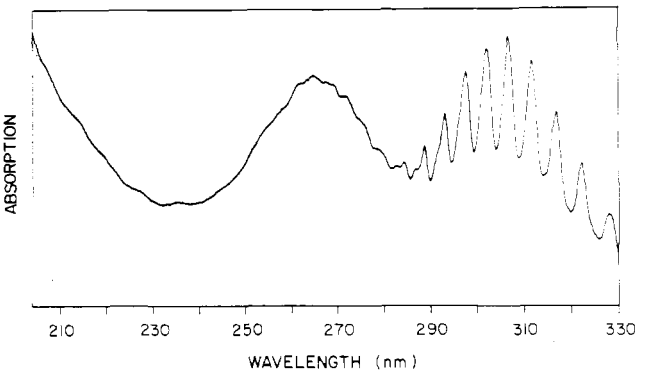

Figure 6. Absorption spectrum of a Rb_2PtF_6–Rb_2SiF_6 mixed crystal at 5 K between 30 000 and 49 000 cm^{-1} showing vibronic structure for the $\Gamma_1(^1A_{1g}) \rightarrow \Gamma_5(^1T_{2g})$ transition at 38 000 cm^{-1}. The $\Gamma_1(^1A_{1g}) \rightarrow \Gamma_4(^1T_{1g})$ transition is also shown at 32 500 cm^{-1}.

Crystal Field Results. Figure 6 shows the absorption spectra at liquid-helium temperature of a Rb_2PtF_6–Rb_2SiF_6 mixed crystal between 30 000 and 49 000 cm^{-1}. Unlike the results in our previous PtF_6^{2-} paper, the $\Gamma_1(^1A_{1g}) \rightarrow \Gamma_5(^1T_{2g})$ transition has now been observed with some evidence of vibronic structure. If the experimental absorption maxima are fitted to the crystal field model discussed previously,[2] the results are consistent with J–T activity for the $\Gamma_3(^3T_{1g})$ electronic state. First, the crystal field calculated energy of the $\Gamma_3(^3T_{1g})$ state is about 2000 cm^{-1} greater than the actual experimental energy; this is due to J–T lowering of the lower potential surface. Incidentally, some evidence of structure appears in the absorption spectrum about 3000 cm^{-1} above the absorption structure at 22 440 cm^{-1}[2] assigned to the lower $\Gamma_3(^3T_{1g})$ potential surface, and this may be due to a transition to the upper $\Gamma_3(^3T_{1g})$ potential surface. Second, when the $\Gamma_1(^1A_{1g}) \rightarrow \Gamma_5(^1T_{2g})$ transition energy is included in the crystal field analysis, a calculated spin–orbit parameter of about 1700 cm^{-1} results, which is much less than expected. This low spin–orbit value indicates the Ham effect is important in the PtF_6^{2-} case. That is, the J–T effect acts to reduce the magnitude of the spin–orbit coupling. It is important to note that other excited states of PtF_6^{2-} may show J–T activity such as the $t_{2g}^5e_g$ $\Gamma_4(^1T_{1g})$ state.

Summary

We have demonstrated the existence of Jahn–Teller activity in the $\Gamma_3(^3T_{1g})$ lowest excited state of the PtF_6^{2-} ion by analysis of an e_g-type progression in the luminescence spectra and comparison with 5 K Raman results. Measurements of the luminescence spectra, lifetimes vs. temperature, and Raman spectra for *both* pure and mixed crystals indicate these systems show the same extent of $\Gamma_3(^3T_{1g})$ Jahn–Teller activity, demonstrating the relevance of mixed-crystal experiments in understanding pure materials. It has been possible to deduce the geometry of the PtF_6^{2-} ion in the $\Gamma_3(^3T_{1g})$ J–T excited state.

Acknowledgment. Research at the University of Maine was supported by NSF, Department of Materials Research, Grant DMR 77-07140. Research at Brookhaven National Laboratory was supported by the Division of Basic Energy Sciences, Department of Energy, under Contract No. EY-76-C-02-0016.

Registry No. Cs_2PtF_6, 16923-85-6; Cs_2SiF_6, 16923-87-6; Cs_2GeF_6, 16919-21-4; Rb_2SiF_6, 16925-27-2; Rb_2PtF_6, 16949-76-1; PtF_6^{2-}, 16871-53-7.

(11) A. Messiah, "Quantum Mechanics", Wiley, New York, 1961, p 433.
(12) R. B. Wilson and E. I. Solomon, *Inorg. Chem.*, **17**, 1730 (1978).
(13) I. N. Douglas, J. V. Nicholas, and B. G. Wybourne, *J. Chem. Phys.*, **48**, 1415 (1968).